The Design and Analysis for Shaped Charge Liner Using Taguchi Method

Jen-Hsin Ou, Jen-Bing Ou, Yan-Jing Jhu

Abstract—In order to study the shaped jet penetration effect on steel plate after the detonation of shaped charge on armor-piercing projectile, the finite element analysis software is used to do the numerical simulation for liner structure analysis from initiation jet forming to penetrating target plate[1]. In this paper, the liner structural parameters, including cone angle, wall thickness, standoff, detonation point, and their effects on Sunder are also analyzed, and finally the Taguchi method analysis is used to study the influence of various factors on jet forming process and find the optimal solution for effective penetrating depth. The results show that the initiation point contributes nearly 22.61% effect on perforating depth and is the most significant factor. The penetrating effect decreases as the initiation point moves from edge to the center. The wall thickness accounts for 11.09% effect on perforating depth. Based on the results above, we can do a better shaped charge liner design in the subsequent application.

Keywords—Liner, Taguchi Method, Jet, Finite Element Analysis

I. INTRODUCTION

THE primary warhead used for armor-piercing projectile is the shaped charge. According to the forms and armor-piercing approaches, there are two types of warhead: explosively formed projectile (EFP), and shaped charge projectile, describing as following.

EFP is also called self-forging fragment (SFF), which is similar to the structure of shaped charge projectile. The main difference between them is that the shaped charge liner of the former is in the shape of a shallow dish, and the blast force moulds the liner into head-covered or rear-covered spherical shape. The mass of the formed warhead is almost equal to that of the shaped charge liner, and every part moves at the same velocity. The aperture caused by the projectile penetrating the armor is large and shallow.

The shaped charge projectile is a device at the end of a concave metallic which the liner is installed. When the fore-end is detonated, the blast waves crash the shaped charge liner axially with great speed, and cause the liner to deform, collide and squeeze along the axis, then converging into a metallic jet with high velocity. Although the mass of charge accounts for only 15% of the total mass of shaped charge liner, the armor-piercing ability of the shaped charge warhead depends on it. Because different parts of the jet travel at various speeds, the jet will stretch itself while flying. The armor will be pierced, providing that the velocity of the shaped charge is greater than the terminal speed for piercing the target. The aperture caused by shaped charge warhead is narrow and long, the velocity and mass of shaped charge will influence the armor-piercing effect. In addition, the cone angle, thickness of wall, and external form of the liner affect the shape of jet. The speed and mass of liner are also the key factors affecting the armor-piercing effect [1].

The appropriate parameters must be found through tests in the process of engineering to determine the shape of shaped charge liner to be applied practically. With the rapid development of computer and numerical simulation technique [2], it has become an important tool to observe the formation process of shaped charge and study on its structural parameters. This paper uses LS-DYNA to carry out the numerical simulation for process of shaped charge jet, exploring the distinction and regularity of jets in different parameters.

II. BASIC THEORIES

A. The Theory of Shaped Charge Jet Penetration

The process from explosion to piercing armor is very complicated and can be divided into four stages. The first one is the explosion caused by explosives, propelling the shaped charge liner forward axially. At this time, it is the property of explosives that takes effect. At the second stage, units of shaped charge liner travel axially, i.e. crashing process. In this process, utter deformation and violent collision occur, causing the jet and the carrot. At the third stage, the jet moves and stretches, and then breaks due to the velocity gradient increasing in the direction of the jet stretch. The jet impacts the target plate at the fourth stage, creating millions unit of atmospheric pressure, sending shock waves from the point of impact to target plate and jet. With its high temperature, high pressure and high-strain-rate areas, the jet bursts apart the target plate, or the armor [3].

Jen-Hsin Ou has gotten a Ph.D in mechanical engineering from Graduate Institute of Mechanical and Electrical Engineering, National Taipei University of Technology. He is a leader of Chung-Shan Institute of Science and Technology Armaments Bureau, MND, System Manufacturing Center. His email is jenhsin.ou@gmail.com, and his cell phone number is +886-922-754-030

Jen-Bing Ou is a Ph.D. Graduate student of Department of Electronics Engineering, Management Information, National Kaohsiung University of Applied Sciences. His email is mailto:jen.bing@msa.hinet.net, and his cell phone number is +886-910-753-062

Yan-Jing Jhu is a Graduate student of Graduate Institute of Manufacturing Technology, National Taipei University of Technology. His cell phone number is +886-935-019-197

B. The Basic Theory of Finite Elements

The principal simulation methods applied in explosion and impact effects include finite element method, finite difference method, and finite volume method [4].

The finite difference method can be divided into the flowing steps: establishing differential equations (control equations), using a mesh to cover space domain and time domain, replacing the differential in the control equation with difference approximation, and then conducting numerical calculation to get the approximate numerical solution. The finite element method can be divided into the flowing steps: to divide the continuous solution domain into finite elements, to assemble a discrete model, and then to calculate the approximate numerical solution. This method is suitable for calculating strong dynamic load questions with complex borders or material interface. It has been developed rapidly and is applied widely in the simulating calculation of impact-related questions. The finite volume method is to transform a partial differential equation into an integration model in physical space, and directly discrete the integration-form law of conservation on the selected control volume in physical space.

Different mesh generation method is selected to establish the equations determine different numerical calculation procedures. There are two calculation methods: Lagrange's method and Euler's method.

The mesh generation used in Euler's method is fixed in space. The material filling the Euler's mesh space is divided into many discrete elements by Euler's mesh. The method is applied to dealing with questions related to great deformation, especially the questions concerning hypervelocity impact, which only can be solved by Euler's method. However, the interface between different matters needs to be dealt with specifically. A complex question needs to be calculated by using relatively large number of meshes, consuming much more computer processing time to solve it.

The mesh used in Lagrange's method is fixed on the object, moving with it. The mesh calculated fixes on the material and deforms along with the material. It can precisely trace the boundaries of and interfaces between materials, so the number of mesh needed is relatively less. However, when a great deformation occurs, the correct result will not be necessarily obtained. Sometimes negative mass, negative volume or other phenomenon would be produced, making finishing the calculation impossible.

III. Shaped Charge Design

The design of liner, including the main body of armor-piercing shaped charge jet, should be optimized from its cone angle, wall thickness, detonation method, and material technology.

Because the diameter of liner will vary with the change of angle and the wall thickness, the liner is adopted by 44° cone angle, 1.05 mm wall thickness and 65 mm diameter.

A. Structural Form of Liner

Usually, shaped charge liners are classified as single cone, double cone, trumpet, and single cone trumpet in shape. In this study, a single cone liner is adopted because it is made easily and a clear contrast can be presented in experiment.

B. The Cone Angle of Liner

For the fixed length, ideal and incompressible fluid theory, the speed of jet decreases with the increase in the cone angle of liner [5], and the mass of jet increases with the increase in the cone angle. Unlike EFP, the selected cone angle is between 30°-70°.

C. The Wall Thickness of Liner

The choice of the liner wall thickness depends on the geometric structure and material of liner, and the characteristics of the jet depend on the expected conditions of use [6]. Generally, the optimal wall thickness will increase as the cone angle and the caliber of liner increase, but decrease as the material density decreases. The influence of material on the shaped charge liner is not taken into consideration, so the influence of the wall thickness is easy to be figured out. The liner is made of red copper. The wall thickness is between 0.7% -2.3% compared to that of the liner diameter.

D. Standoff

Standoff refers to the vertical distance between the bottom of the liner and the target plate. It affects the extent which the shaped charge jet can penetrate the target plate. As the explosion is ignited, a jet is formed. The standoff length affects the shape of the jet when contacting the target plate [7]. The suitable shape is conducive to penetrate into target plate. In this study, the ranges of standoffs are the values that from 1-9 multiply by the liner diameter. The experimental parameters are used as basic model data, and we hope that how the standoff parameter will affect the armor-piercing depth will be found.

E. Detonation Point

In view of the influence of detonation point of explosion, several detonation points are considered in this study by using the same amount of explosive, including the point at the center, the point in the middle, and the point on the margin. Because the angles and wall thicknesses are different, the structures in each group are different, so are the radii of explosive. To maintain the same amount of explosive, the height of the explosive structure for each group will be changed accordingly, and the detonation points are determined in accordance with the relative points of the group.

IV. The Results and Discussion on the Formation of Shaped Charge Jet

A. Single Factor Experiment

As mentioned above, there are many factors that affect the armor-piercing ability, such as the material of explosive or liner, cone angles, and wall thickness. Because the purpose in this

study is to carry on an experiment on the factors of liner's structure and discuss the manufacturing feasibility, this study will analyze cone angles, standoffs and detonation points as factors [8,9], shown as following:

Cone angles: 43°, 44°, 45°, 46°, 47°

Wall thickness (mm): 0.05, 0.75, 1.05, 1.35, 1.60
Standoff (x times caliber): 1, 3, 5, 7, 9
Detonation point: center point, middle point, marginal point

1. The Simulation Planning for Geometric Parameters of Model

The geometry of model is set up by using CAD software. Because the purpose is to analyze the armor-piercing depth, the original model is simplified to a 1/2 plate modeling, as shown in Fig 1. The fixed area of explosives domain is 3200 mm^2, where a represents the cone angle of liner, b represents the wall thickness of liner, and c represents standoff.
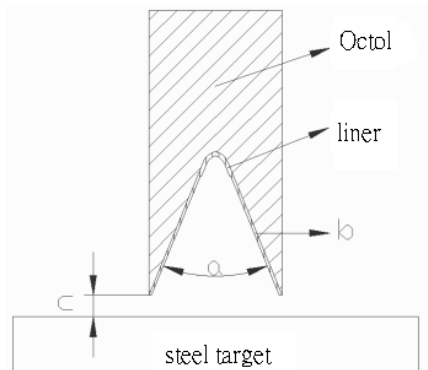

Fig.1 the Diagram of Model

The detailed size of shaped charge liner is shown in Fig 2, where a represents its cone angle, and b represents its wall thickness.
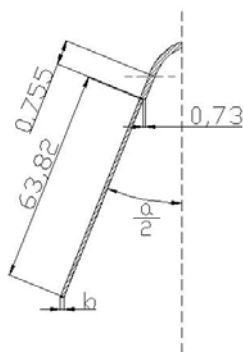

Fig.2 The diagram of shaped charge liner model (unit: mm)

2. Material Parameters and the Types of Finite Elements

The explosive is made of Octol 178/22 and high-explosive-burn is used in ANSYS. The main parameters are shown as Table 1.

Table.1 Octol 178/22

Explosive (Octol 178/22)	
Density	0.001821g/mm3
Detonation Velocity	8.48 mm/μs
Pcj Pressure	29.37 GPa

The shaped charge liner is made of red copper that is a kind of metal with high ductility. Johnson-Cook material model is used. Gruneisen equation of state is used to describe the reaction under dynamic action. The main material parameters are shown in Table 2.

Table.2 Red Copper Material Parameters

Shaped Charge Liner (Red Copper)	
Density	0.00896g/mm3
Elastic Modulus	40 GPa
Poisson's Ratio	0.35
Melting Point	1356 K

Null is adopted as air material, and the state equation is Gruneisen.

The target plate is made of AISI 1010 Steel, using Plastic-Kinematic material model. The parameters are shown as Table 3.

Table.3 AISI 1010 Steel Material Parameters

Steel Target (AISI 1010 Steel)	
Density	0.00787g/mm3
Elastic Modulus	205 GPa
Yield Strength	305 MPa
Tensile Strength	365 MPa
Poisson's Ratio	0.29

3. Mesh Planning

Because there are a serious of mesh deformations occurring

in the process of explosion and penetration, the ALE calculation method provided by ANSYS/LS-DYNA software is applied in the study to calculate the jet penetration. There are two kinds of calculations methods, Lagrange's method and Euler's method, which can be used to calculate mesh deformation and EFP formation process related to material flow. Euler's method is used to calculate multi-material flows, such as explosive occurs between shaped charge liner and air [10]. Lagrange's method is used to calculate the deformation of target plate.

The size of mesh used for explosives that occur between shaped charge liner and air is 0.5 mm, and the 60 progressive meshes model is used for the target plate (meshes become smaller from fringe to center). The thickness is 0.3 mm and divided into 3 sections. Fig 3 shows the ANSYS mesh generation in control group.
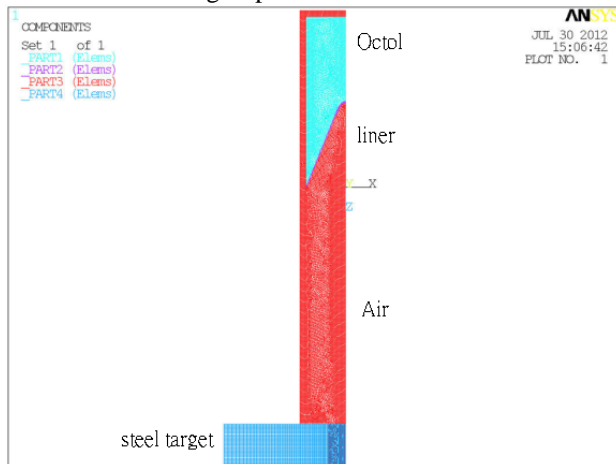

Fig.3 Mesh generation for finite elements in control group

4. *Boundary Conditions Setting*

The setting of boundary conditions is very important for simulation engineering and whether the setting conforms to the real physical phenomenon is critical. Wrong settings usually lead simulation to unreasonable results.

For the 1/2 model, a displacement constraint in X direction is placed along the symmetric axis, as shown in Fig 4.
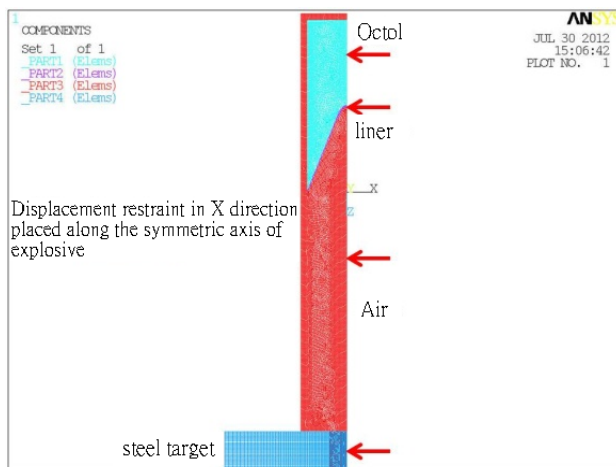

Fig.4 Boundary Setting (1)

Displacement restraint in X direction placed along the symmetric axis of explosive, shaped charge liner, air, and target plate.

In the deformation process of explosive jet, the shape of model is transformed from a cylinder into a plate [11], and its penetration destruction will not act on Y axis, as shown in Fig 5.
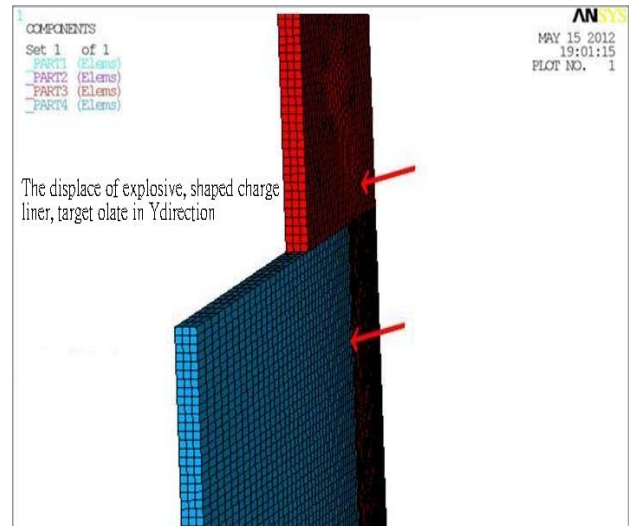

Fig.5 Boundary setting (2)

The displacements of explosive, shaped charge liner, and target plate are in Y direction.

On the other hand, the target is fixed on the same place, which will not move in the process of penetration, as shown in Fig 6.
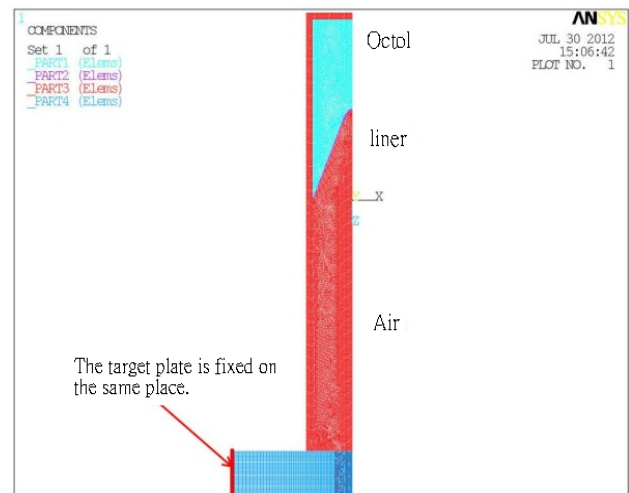

Fig.6 Boundary setting (3)

5. *Simulation analysis of armor-piercing effect*

The single-factor analysis for each factor with 3 to 5 levels is carried out by using LS-SYNA, and the simulation results [12] for each factor are shown in Table 4. It determines the possible defect of the predicted technology before the part is really manufactured, reducing the costs of preparing production [13].

Table.4 Single Factor Analysis Results

Cone Angle	43°	44°	45°	46°	47°
Armor-Piercing Depth (mm)	272.6	284.2	291.8	275.3	260.4

Wall Thickness (mm)	0.05	0.75	1.05	1.35	1.6
Armor-Piercing Depth (mm)	199.2	213.2	284.2	265.1	259.5

Standoff (X times caliber)	1	3	5	7	9
Armor-Piercing Depth (mm)	250.69	284.4	268.9	234.1	210.6

Detonation Point	Whole Surface	The Point on Verge	Center Point
Armor-Piercing Depth (mm)	284.2	317.6	227.5

B. Design of Experiment Using Taguchi Method

The purpose and property of using Taguchi Method include a target value and the tolerance between the qualified and unqualified one. The design of Taguchi Method experiment is a kind of moderate design based on the foresaid reasons. The most important principle of the method is to obtain maximum experimental results and conduct those with minimum experiments. Therefore, Taguchi Method experiment is an effective design principle for experiment.

1. The Design of Experiment

In this experiment, 4 control factors and 3 interactions are used at 3 levels, and the $L_{27}(3^{10})$ orthogonal array is applied.

The test levels of these 4 control factors are defined as follows:

Factor A: 3 different cone angles of the liner, respectively as
  44°, 45°, and 46° [14]

Factor B: 3 different wall thicknesses, respectively as 0.9mm,
  10.5mm, and 1.2mm

Factor C: 3 different standoffs (X times caliber) are multiples
  of 65 mm applied in the control group, values
  respectively as 2, 3, and 4

Factor D: three different detonation points, center point,
  marginal point and middle point

Interaction: observing the interaction between the wall thickness and other factors, including B×A, B×C and B×D.

2. The factor effects analysis of design for experiment using Taguchi method

Taguchi method [15] uses orthogonal array to conduct parameters design and evaluates the standard of parameter levels by signal-to-noise (S/N) ratio. The principle of parameter design is to put controllable factors in the inner orthogonal array and make confounding factors the outer orthogonal array. The test is carried out on the intersection between the inner and outer orthogonal array. According to the types of quality characteristics, the loss function is used to find out S/N ratio, then transforming the quality characteristics obtained by experiment into S/N ratio [16].The analysis is then carried out. Finally, the optimal parameter level combination will be achieved according to statistic deduction [17].

$$(S/N)_{LB} = -100 \log \frac{\sum_{i=1}^{n} \frac{1}{y_i^2}}{n} \tag{1}$$

Table.5 S/N Ratios

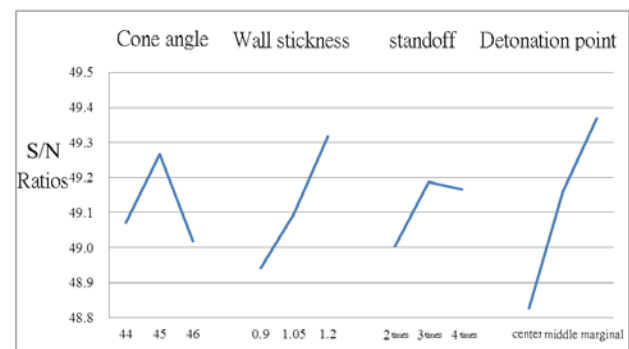| Experiment Code	Cone angle	Wall Thickness	Standoff	Detonation Point
	A	B	C	D
Level 1	49.020	48.892	48.953	48.777
Level 2	49.217	49.046	49.136	49.319
Level 3	48.969	49.268	49.117	49.109

Fig.7 The reaction of controlling factors on S/N ratio

For the three levels of facto A, the difference between the ratio values is small. The S/N ratio value of A₂, 49.217dB, is the largest one, which means the armor-piercing effect is the largest

at 45°, but slightly different at 44°. The armor-piercing effect will be decreasing when the angle is greater or smaller than 45°, and the armor-piercing effect at 44° is larger than that at 46°, as shown in Fig 7.

Fig 7 shows that the armor-piercing effect is the optimal among the three levels of factor B when the wall thickness is 1.2mm. The S/N ratio value is 49.268 dB. The armor-piercing effect decreases with the decrease of wall thickness. The S/N ratio value is 48.892 dB when the wall thickness is 0.9 mm. According to Fig 7, the ratio values present a linear development.

The S/N ratio is 48.953 dB at level 1 of factor C, the smallest among the three levels, and the related length is 130 mm. The largest S/N ratio value is 49.136 dB at level 2 when the explosion height is 3 times the caliber, which is 195 mm long.

As shown in Fig 7, it is easy to find that the factor D related effect is optimal when the explosives are detonated at the marginal point. The S/N ratio value is 49.319 dB. On the other hand, the effect is worst when the explosion point is at center. The S/N ratio is 48.777 dB. The armor-piercing effect is decreasing when the explosion point the moves from margin to center.

Finally, according to the result of the S/N ratio chart, the optimal combination of parameters (cone angle, wall thickness, explosion height, and detonation point) will affect armor-piercing effects. The higher signal means the better quality characteristics. According to Fig 7, when the combination of parameters is $A_2B_3C_2D_2$, the optimal armor-piercing effect can be achieved. A2 refers cone angle to be 45°; B_3 means the wall thickness to be 1.2 mm; C_2 indicates the explosion height to be 3 times the caliber; D_2 points out that the explosion point is at the margin. And the optimal S/N ratio value of parameter is 49.736 dB.

3. Analysis of Interaction Effect

According to Taguchi method, if a factor changes along with the setting level of other factor, these two factors interact with each other [18].

This study also conducts analysis of S/N ratio for the interaction between B factor and other factors, as shown in Table 6.

Table.6 Interaction S/N Ratios

Level	B×A	B×A	B×C	B×C	B×D	B×D
1	48.778	49.207	49.125	49.075	49.164	48.958
2	49.292	48.915	48.921	48.939	48.898	49.118
3	49.136	49.804	49.16	49.192	49.143	49.129

If the two line segments concerning two factors are not parallel with each other in interaction diagram, there is interaction between them. On the contrary, if they are parallel with each other, there is no interaction. The larger the cut angle between the two lines, the larger the interaction between them will be. If a generalized linear model is adopted in experiment, the interaction is equal to the product of the two factor variables. We can easily find that the product of B×A and B×C is significantly larger than that of B×D, as indicating in Table 6. For B×A column, the product of B_3A_3 has the largest S/N ratio value, which is 49.530 dB. Among products of B×C, the B_3C_2 has the largest S/N ratio value, which is 49.515 dB. Among products of B×D, the B_3D_2 has the largest S/N ratio value, which is 49.560 dB.

According to the results of interaction, the combination $A_3B_3C_2D_2$ has the optimal S/N ratio with the most effective armor-piercing force when the cone angle is 46°, the wall thickness is 1.22mm, the explosion height is 3 times the liner caliber, 195 mm long, and the detonation point is at the margin. The related S/N ratio value is 50.069 dB.

The difference between the S/N ratio values and the interaction is 0.333 dB. So, the influence of interaction cannot be ignored.

C. Analysis of Variance (ANOVA)

Because there are different degrees of influence caused by different factors, the AVOVA will be conducted to explore the different degrees of influence, as shown in Table 7.

Table.7 AVOVA of Armor-Piercing Depth

Factors	SS	DOF	Var	F	Confidence
A	297.98	2	148.99	1.74	4.77%
B	693.25	2	346.63	4.04	11.09%
C	227.14	2	113.57	1.32	3.63%
D	1413.78	2	706.89	8.24	22.61%
B×A	1317.41	2	658.71	7.68	21.07%
B×A	529.29	2	264.64	3.08	8.46%
B×C	331.93	2	165.96	1.93	5.31%
B×C	312.52	2	156.26	1.82	5.00%
B×D	432.28	2	216.14	2.52	6.91%
B×D	182.50	2	91.25	1.06	2.92%
Error	514.78	6	85.80		8.2%
Total	6252.85	26			

Factors	SS	DOF	Var	F	Confidence	Significance
A	297.98	2	148.99	1.607	74.09%	No
B	693.25	2	346.63	3.738	92.86%	No
C						
D	1413.78	2	706.89	7.622	98.60%	**Yes**
B×A	1846.70	4	461.67	4.978	97.40%	**Yes**
B×C	644.45	4	161.11	1.737	76.55%	No
B×D	614.77	4	153.69	1.657	74.85%	No
Error	741.92	8	92.74			
Total	6252.85	26				

According to Table 7, factor D is the most significant, which is 22.61%, the second is factor B, which is 11.09%, factor C is 4.77%, and factor D is 3.63%. It is obvious that cone angles have little effect on armor penetration.

For the influence of interaction, because three levels Taguchi experiment demands for four degrees of freedom (DOF), the number of interaction should be divided by 2, and with the same DOF, the contribution difference between them can be distinguished. By calculating, the contribution of B×A is 14.76%, B×C is 5.16, and B×D is4.92%.

The interaction between B and A account for 14.76%, which cannot be neglect. The interaction between B and D is the second, accounting for 5.16%. The interaction between B and C accounts for is only 4.92%.

The contribution factors that smaller than 4% are regarded as error items. The confidence levels over 95% are significant, as shown in Table 8.

Table.8 S/N Statistic Error of Armor-Piercing Effect

According to Table 8, the result of statistic error of penetration depth shows that at 95% confidence level, only the armour-piercing effects D and B×A are significant, and the confidence levels are 98.6% and 97.4% respectively.

When considering the impact of 4 factors, including cone angle, wall thickness, Standoff, and denotation point, it shows that the optimal combination of factors using Taguchi method is $A_2B_3C_2D_2$. Its S/N ratio value is 49.736 dB. The predicted armor-piercing depth is 306.76 mm, as shown in Fig 8.
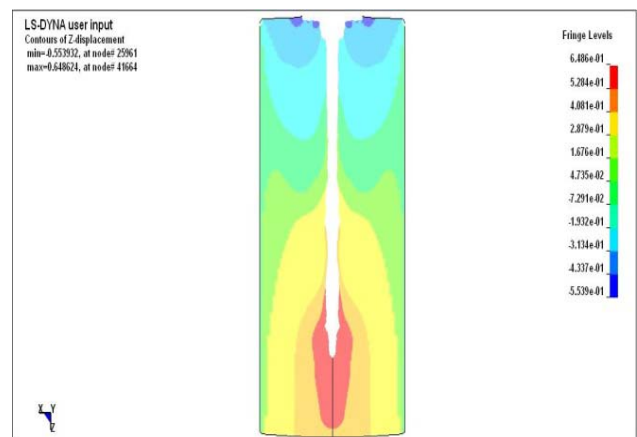

Fig.8 the simulation diagram of the combination of factors A2B3C2D2

Taking interaction, including B×A, B×C and B×D, into consideration, , the optimal combination of factors is $A_2B_3C_2D_2$, and the S/N ratio value is 50.069 dB. The predicted armor-piercing depth is 318.75 mm, as shown in Fig 9.
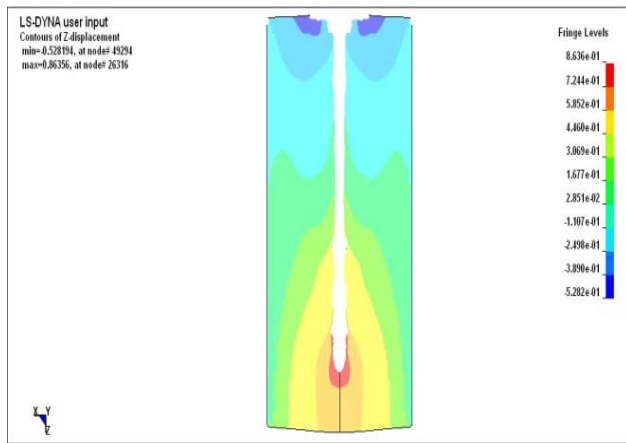
Fig.9 the simulation diagram of the combination of factors $A_3B_3C_2D_2$

Table.9 the comparison between two optimal simulation results

Combinations of Factors	S/N Ratio (dB)	Predicted Depth (mm)	Simulation Results (mm)	Error Rate (%)
$A_2B_3C_2D_2$	49.736	306.76	303.47	1.084
$A_3B_3C_2D_2$	50.069	318.75	320.12	0.428

According to Table 9, the simulated penetration depth of the optimal combination, $A_2B_3C_2D_2$, is 303.47 mm, with only 4 factors being taken into consideration. If the interaction is also taken into consideration, the optimal combination is $A_3B_3C_2D_2$, with armor-piercing depth to be 318.75 mm.

Furthermore, without considering interaction, the error value of the combination is larger. That indicates that it is enough for the simulation experiment to analyze four factors [19], and the prediction will be more accurate by adding the interaction to do analysis.

V. CONCLUSION

When the same material and amount of explosive are used, four control factors, including cone angle, wall thickness, standoff and detonation point, are selected in this FEM study [20,21], with three levels for each factor. The Taguchi experimental method and ANOVA table are used to analyze and determine the optimal condition. According the experiment, the following results are achieved to improve the armor-piercing effect of shaped charge liner.

1) When taking the 4 factors into consideration, including A (cone angle), B (wall thickness), C (standoff), D (detonation point), and with 3 levels for each factor, the most influential factor is D, which accounts for 22.61% impact. B comes the second, and then A the third.

2) The armor-piercing effect is the best when the cone angle is 45°. The armor-piercing effect will be decreasing when the angle is greater or smaller than 45°. According to the results, the armor-piercing effect at 44° is larger than that at 46°. So, it is predicted that the increase gradient of decreasing angles is larger than increasing angles.

3) For 3 different levels, the thicker the wall, the better the effect will be. When the explosion height is 3 times caliber, there will have the best armor-piercing effect.

4) For three detonation points, including center, middle and marginal point, to detonate the explosive at marginal point can produce the best effect. The armor-piercing effect will be decreasing when the explosion point moves from margin to center.

5) For the influence of interaction, there will be B×A> B×C> B×D. The interaction between B and A accounts for 14.76%, which allows no neglect. The influences of B×C and B×D are relatively small.

6) The factors contribution those are smaller than 4% are regarded as error items. The confidence levels over 95% are significant. After the 4 factors with 3 levels are analyzed, only the two armor-piercing effects, D and B×A, are significant.

7) According to the results of optimal simulation, it shows that the interaction actually influence the experimental results in the study. So, the interaction between factors must be taken into consideration.

REFERENCES

[1] Li Na Cao, Siou Cing Han, Siao Gang Dong, Yong Guang Jhang, The numerical simulation for control blasting and Armor-Piercing process, Journal of Science and Engineering, vol 9, No 23, 2009.

[2] Li Sin Syu, Syong Cao, Song Cheng, Yang Sun, Numerical Simulation of Ring Initiation for Shaped Charge, Journal of North University of China ,vol 30, No 5, 2009.

[3] Jian Fu Ma, Study on the Mechanism of Penetrating into Concrete Using Shaped Charge Structures, North University of China, Weapon system and application engineering, Master' s dissertation , 2007.

[4] De Gun Wang, A study of selectable EFP penetration forming, Nanjing University of science and technology, Master's dissertation of automatic weapon and ammunition, 2007.

[5] Yang Jhao, A study of cavity liner, Nanjing University of science and technology, Master's dissertation of automatic weapon and ammunition, 2006.

[6] Ai Pin Fei, Yun Jyun Guo, Numerical simulation of linear shaped charge jet with uneven thickness cover, Engeering Blasting, vol 13, No 1, 2007.

[7] Rong Guei You, Guo Huang Chen, Research of the warhead of armor-piercing rock, Hsin Hsin Quarterly, vol 37, No 3, p53-58 , 2010.

[8] O. Ayisit, The influence of asymmetries in shaped charge performance, International Journal of Impact Engineering, vol. 35, pp. 1399–1404, 2008.

[9] Adam Jackowski, Edward Włodarczyk, The influence of repressing liners made from sintered copper on jet formation, Journal of Materials Processing Technology, vol. 171, pp. 21–26, 2006.

[10] M. Huerta, M.G. Vigil, Design, Analyses, and field test of a 0.7m conical shaped charge, International Journal of Impact Engineering, No 32, pp.1201-1213, 2006.

[11] W. Guo, S.K. Li. F.C. Wang and M. Wang, Dynamic recrystallization of tungsten in a shaped charge liner, Scripta Materialia, vol. 60, pp.329–332, 2006.

[12] Ryo Kagaya, Masayuki Ikebe, Tetsuya Asai, and Yoshihito Amemiya, On-Chip Fixed-Pattern-Noise Canceling with Non-Destructive Intermediate Readout Circuitry for CMOS Active-Pixel Image Sensors, WSEAS TRANSACTIONS on CIRCUITS AND SYSTEMS Issue 3, Volume 3, May 2004, pp.477-479

[13] Alexandru C. FILIP, Ion NEAGOE, Simulation of the Metal Spinning Process by Multi-Pass Path Using AutoCAD/VisualLISP, 3rd WSEAS International Conference on Engineering Mechanics, Structures, Engineering Geology, 2010, pp.161-165.

[14] Tong Sheng Sei, Jen Hsin Ou, Research of armor-piercing liner, Hsin Hsin Quarterly, Volume 40, No 4, 2012, pp.88-94.

[15] Y.F. Hsiao , Y.S. Tarng, K. Y. Kung, Application of Grey-based Taguchi methods on Determining Process Parameter of linear motion guide with Multiple Performance Characteristics, 11th WSEAS International Conference on APPLIED MATHEMATICS, Dallas, Texas, USA, March 22-24, 2007, pp.72-79

[16] Seokbin Lim, Steady state equation of motion of a linear shaped charges liner, International Journal of Impact Engineering, vol. 44, pp. 10-16, 20.

[17] CARLOS M. VÉLEZ S., ANDRÉS AGUDELO, Control and parameter estimation of a mini-helicopter robot using rapid prototyping tools, WSEAS TRANSACTIONS on SYSTEMS Issue 9, Volume 5, September

[18] Huei Huang Li, Taguchi Methods: Principles and Practices of Quality Design, Gau Lih Book Co. 2011

[19] Ondina Popescu, Hector Marin, Cezar Popescu, Javier Quezada, Joao Ofenboeck, Juan Cortes, The industry faculty connection using a failure analysis process, WSEAS TRANSACTIONS on CIRCUITS AND SYSTEMS Issue 3, Volume 3, May 2004, pp.581-586

[20] Su-Hai Hsiang, Yi-Wei Lin, and Wen-Hao Chien, Investigation of Experimental and Numerical Analysis on Extrusion Process of Magnesium Alloy Fin Structural Parts, WSEAS International Conference on Geography, Geology, Energy, Environment and Biomedicine, August 2011, pp.300-305.

[21] F. Neri, Software Agents as A Versatile Simulation Tool to Model Complex Systems. WSEAS Transactions on Information Science and Applications, WSEAS Press (Wisconsin, USA), issue 5, Vol. 7, 2010, pp.609-618.